4.0 THERMOELASTIC STABILITY.

The thermoelastic problems considered in the previous paragraphs have followed formulations of the linear theory of thermoelasticity; they have thus excluded questions of buckling, problems in which the effect of the loading depends on the deformations (as in the case of beam-columns), large deflections, and other similar effects. It is the purpose of this paragraph to discuss some of the principal problems of this type. It should be remembered that the solutions are approximate from the viewpoint of an exact thermoelastic formulation. The nature of these approximations was treated in the previous subsections.

4.0.1 Heated Beam Columns.

If a beam-column is subjected to the action of heat, the influence of temperature must, in general, be taken into account. The analysis in the cases in which the ends of the beam are restrained in the axial direction is slightly different from that used when the ends are free to displace in that direction. The latter case will be considered in paragraph 4.0.1.1 while the former is considered in paragraph 4.0.1.2.

4.0.1.1 Ends Axially Unrestrained.

The buckling behavior of beams (and therefore also their behavior as beam-columns under any combination of transverse and axial loads) depends on the shape of the cross section: For example, a beam whose cross section possesses no axes of symmetry can buckle only by a combination of twisting

and bending, whereas in other cases some of the uncoupled modes are also possible. The general formulation and solution of this problem are discussed in Ref. 1, but for simplicity, the following analysis is restricted to doubly symmetrical beams, with least principal moment of inertia under a transverse distributed load $p = p(x)$ acting in the xy plane, and subjected to a temperature distribution such that $M_{T_y} = 0$. The beam will thus bend in the xy plane without twisting and with $w = 0$. The governing differential equation is

$$\frac{d^2}{dx^2}\left(EI_z \frac{d^2v}{dx^2}\right) + P \frac{d^2v}{dx^2} = p - \frac{d^2M_{T_z}}{dx^2} \quad . \tag{1}$$

It is convenient to obtain the solution in two parts, by separating the effects of temperature and of transverse load. For this purpose v_T is the deflection the beam would undergo if only temperature and the axial load P were present (transverse loads absent); it therefore satisfies the differential equation

$$\frac{d^2}{dx^2}\left(EI_z \frac{d^2v_T}{dx^2}\right) + P \frac{d^2v_T}{dx^2} = - \frac{d^2M_{T_z}}{dx^2} \quad . \tag{2}$$

The quantity v_p is the deflection the beam would undergo if only transverse loads and the axial load P were present (temperature effects omitted); it therefore satisfies the differential equation

$$\frac{d^2}{dx^2}\left(EI_z \frac{d^2v_P}{dx^2}\right) + P \frac{d^2v_P}{dx^2} = p \quad . \tag{3}$$

With the definitions, the solutions of the combined problem in which all loads are acting is

$$v = v_T + v_P \quad .$$

The component deflection v_P represents the solution of the ordinary isothermal beam-column problem and can often be found in the literature (see Section B4.4). The determination of v_T must, in general, be carried out anew for each new problem. However, in the special case of uniform beam under a temperature distribution of the form of a polynomial of a degree not higher than the third in the spanwise direction, that is, when

$$M_{T_z} = a_0 + a_1 x + a_2 x^2 + a_3 x^3 \quad ,$$

then

$$v_T = -\frac{M_{T_z}}{p} + c_0 + c_1 x + c_2 \sin kx + c_3 \cos kx \quad ,$$

where $k = \sqrt{\frac{P}{EI_z}}$ and the constants c_0, c_1, c_2, and c_3 are determined from the boundary conditions. Solutions for v_T for three important special examples for which

$$M_{T_z} = a_0 + a_1 x$$

are given as follows.

I. Both Ends Fixed.

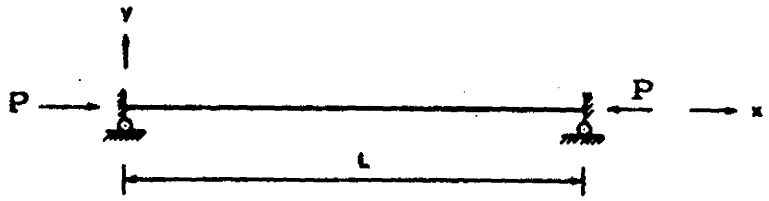

$$v_T = 0 \text{ for } P < P_{cr} = \frac{4\pi^2 EI_z}{L^2} \quad .$$

II. Both Ends Simply Supported.

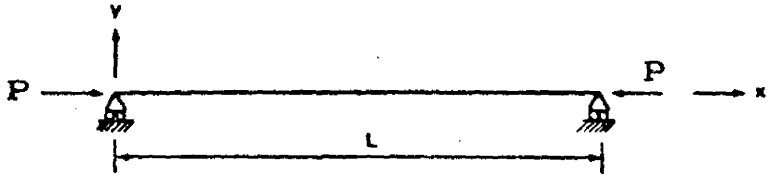

$$v_T = -\frac{a_0}{P}\left(\frac{\cos kL - 1}{\sin kL}\sin kx + 1 - \cos kx\right) - \frac{a_1}{P}\left(x - L\,\frac{\sin kx}{\sin kL}\right)$$

and

$$P_{cr} = \frac{\pi^2 EI_z}{L^2} \quad .$$

III. Cantilever.

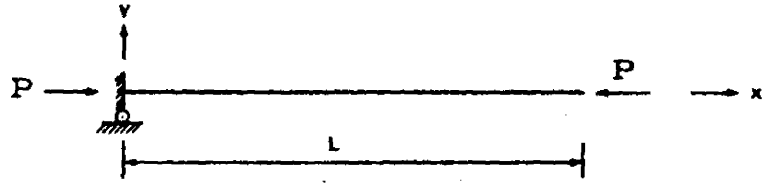

$$v_T = -\frac{a_0}{P}\,\frac{1 - \cos kx}{\cos kL} - \frac{a_1}{Pk}\left[\left(\frac{kL - \sin kL}{\cos kL}\right)(1 - \cos kx) + kx - \sin kx\right]$$

and

$$P_{cr} = \frac{\pi^2 EI_z}{4L^2} \quad .$$

The axial stress is given by

$$\sigma_{xx} = -\alpha ET + \frac{P_T - P}{A} + \frac{y}{I_z}\left(M_{T_z} + M_z + P_v\right) \quad .$$

In these analyses, the beam-column has been assumed to carry a compressive axial load. If the load is tensile, the appropriate results may be obtained by replacing the quantity P by (-P) in the corresponding expressions valid for a compressive load: accordingly, the quantity (k) must be replaced by (ik), (k^2) by ($-k^2$), (sin kx) by (i sinh kx), (cos kx) by (cosh kx), (tan kx) by (i tanh kx), etc. Here $i = \sqrt{-1}$ and the symbol k denotes

$$k = \sqrt{\frac{|P|}{EI_z}} \quad .$$

4.0.1.2 Ends Axially Restrained.

In this case, the basic equation to be solved is still equation (1) of 4.0.1.1, but the magnitude of the load P is unknown and must be determined from an additional condition concerning the axial displacements of the ends. If both ends are rigidly fixed in the axial direction, these conditions shall be stipulated: The axial distance between the ends of the bar must remain unchanged and temperatures must remain constant along the span. Expressed mathematically,

$$(P - P_T)\ \frac{L}{AE}\ + \Delta = 0 \qquad (4)$$

where

$$\Delta = \frac{1}{2}\ \int_0^L\ \left(\frac{dv}{dx}\right)^2\ dx\ . \qquad (5)$$

The analogous condition appropriate to the case in which the ends of the bar are elastically restrained in the axial direction is easily derived. If, for example, the ends are attached to linear springs with modulus K, equation (4) takes the form

$$\left[P\left(1 + \frac{AE}{KL}\right) - P_T\right]\ \frac{L}{AE} + \Delta = 0\ . \qquad (6)$$

The transverse deflection v appearing in the quantity Δ must be calculated by the equations given in the preceding paragraph (4.0.1.1); as a consequence, the analysis of beam-columns which have ends fixed in the axial direction is quite cumbersome, since the unknown P and v must be determined by the simultaneous solution of equations (1) and (6). However, if the temperature is expressed as a polynomial, the calculations are greatly facilitated by the use of a series of graphs in conjunction with a rapidly convergent iteration procedure. This technique and its results are available in Ref. 7 within the following limits:

1. Distributed transverse loads are uniform over the span, whereas concentrated loads are at the midspan.

2. The temperature varies linearly through the depth and is constant in a spanwise direction.

3. The beam is assumed to be simply supported at its ends for bending and elastically restrained axially.

Tables of numerical results in nondimensional form are presented for the cases of zero and full axial end restraint in rectangular beams. These tables may be used to determine maximum deflections and bending moments.

4.0.2 Thermal Buckling of Plates.

4.0.2.1 Circular Plates.

General.

This section contains curves and data based on nonlinear, elastic behavior and involving the use of large-deflection theory. This is because plate stresses and deflections in the post-buckled state represent the major considerations. The basis for this is the well-known fact that certain compression structures can support some increment of additional loading before complete collapse and, in the process of so doing, accept increased stresses and deflections. This can be readily seen by an inspection of the plate buckling stress and allowable compression stress for specific materials, taken as a function of the crippling parameter $(a/t\sqrt{k})$. Particular considerations and background, as developed by Newman and Forray in Refs. 32 and 33, are given in the following paragraphs, along with the solution of an example problem for demonstration of the methods involved.

Configuration.

The design curves and equations provided here apply only to flat, circular plates which are of constant thickness and are made of an isotropic material. It is assumed that the plate is free of holes, obeys Hooke's law, and that Poisson's ratio is equal to 0.3.

Boundary Conditions.

The solution is valid only where both of the following conditions are satisfied:

1. The boundary is simple supported; that is,

$$w = M_r = 0 \text{ at } r = b \quad . \tag{7}$$

2. The middle surface of the plate is radially fixed; that is,

$$\bar{u} = \bar{v} = 0 \text{ at } r = b \quad . \tag{8}$$

Temperature Distribution.

The plate may have a thermal gradient through the thickness, provided that the distribution is symmetrical about the middle surface. However, it is required that the temperature be uniform over the surface. Therefore, the permissible distributions can be expressed in the form

$$T = T(z) \tag{9}$$

subject to the restriction that

$$T(+z) = T(-z) \quad . \tag{10}$$

Obviously, the special case of a plate at uniform temperature complies with these specifications.

Design Curves and Equations.

If a heated plate is constrained against free, in-plane expansion, compressive stresses are developed in the plate. Initial out-of-plane buckling occurs at very low temperature increments in the case of thin plates constrained in this manner. However, in many structural situations, the usefulness of the plate is not completely lost as a result of this initial buckling since it is able to carry some additional load after it has reached the buckled state. In view of this, cases may arise in which a knowledge of the magnitudes of the post-buckled stresses and deflections would be most helpful. To determine the stresses and deflections of a plate after initial buckling has occurred, large deflection theory must be used in the analysis since the actual deflection at that stage may be several times the thickness of the plate.

In Ref. 33 Newman and Forray present a large-deflection analysis of a circular plate under mechanical and thermal loading. Since a closed-form solution of the basic differential equations was not possible, they used a finite-difference procedure to set up the governing differential equations for digital computer solution. Numerical results were then obtained for a wide range of temperature resultants, N_T'. These results are presented in curve form in Figures 4.0-1 through 4.0-5 for deflections, radial and tangential forces, and moments for various temperature gradients, as defined in equations (9), (10), and (16).

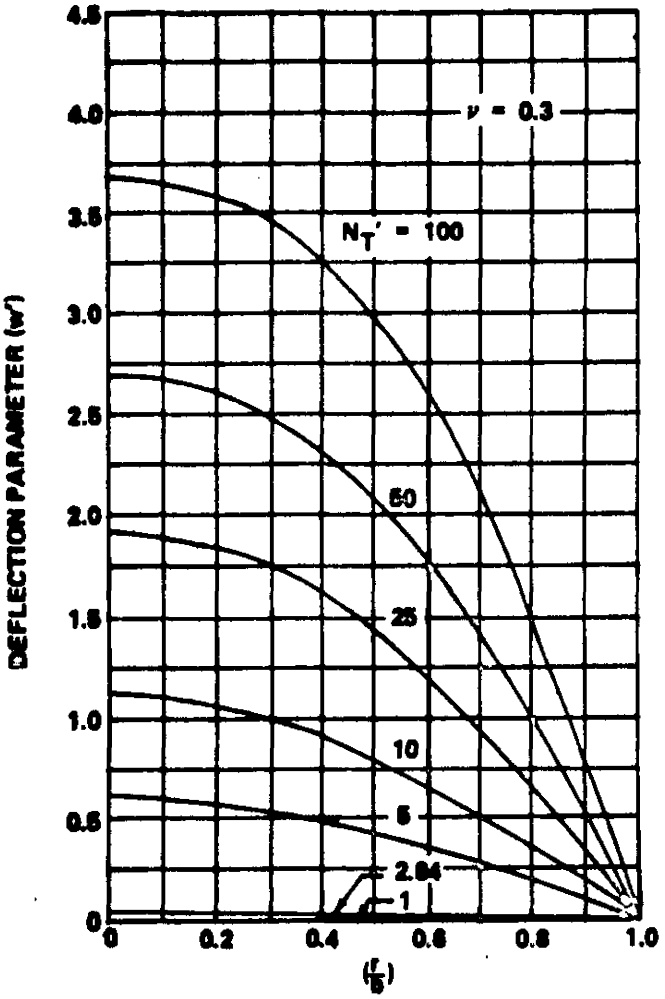

Figure 4.0-1. Nondimensional deflection parameter.

Even though nonlinear analysis methods are used to find the post-buckling deflections and stresses, these solutions hold since it has been shown in Ref. 34 that initial buckling can occur when the edge compressive stress exceeds the lowest eigenvalue of the small deflection buckling problem. Timoshenko [35] shows that this critical compressive stress for a circular plate with $\nu = 0.3$ is given by

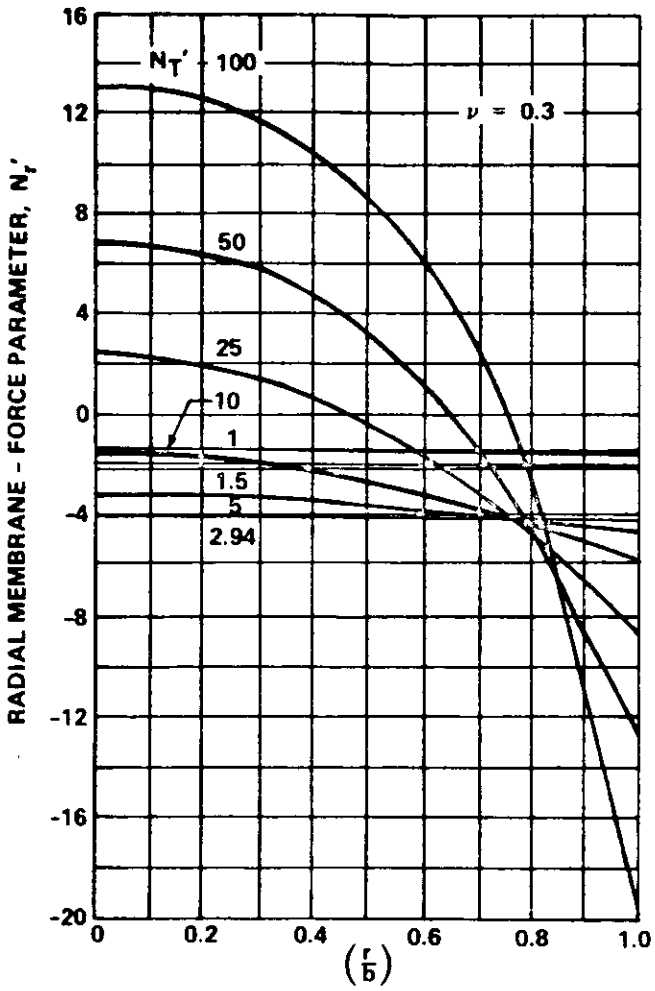

Figure 4.0-2. Nondimensional radial membrane-force parameter.

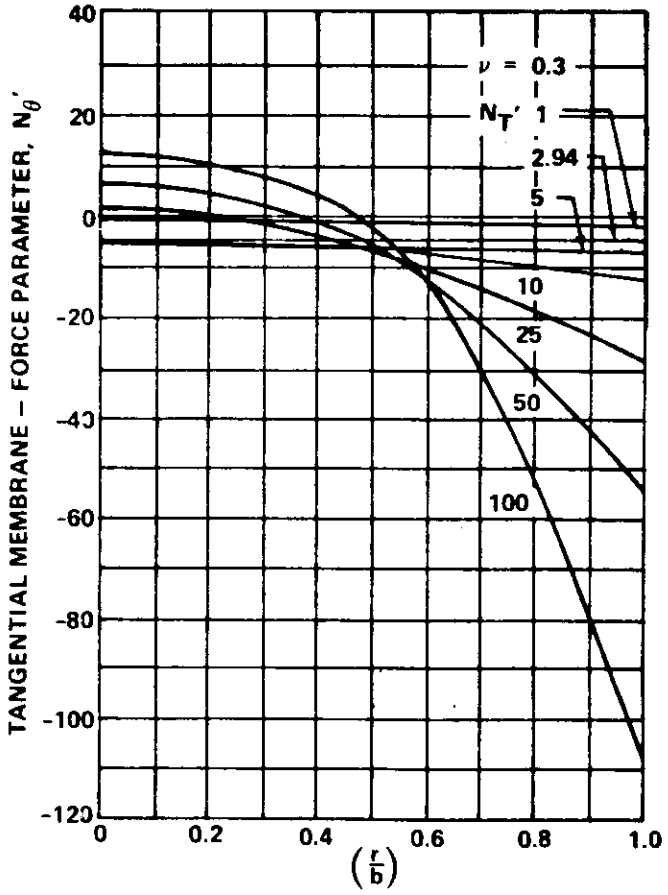

Figure 4.0-3. Nondimensional tangential membrane-force parameter.

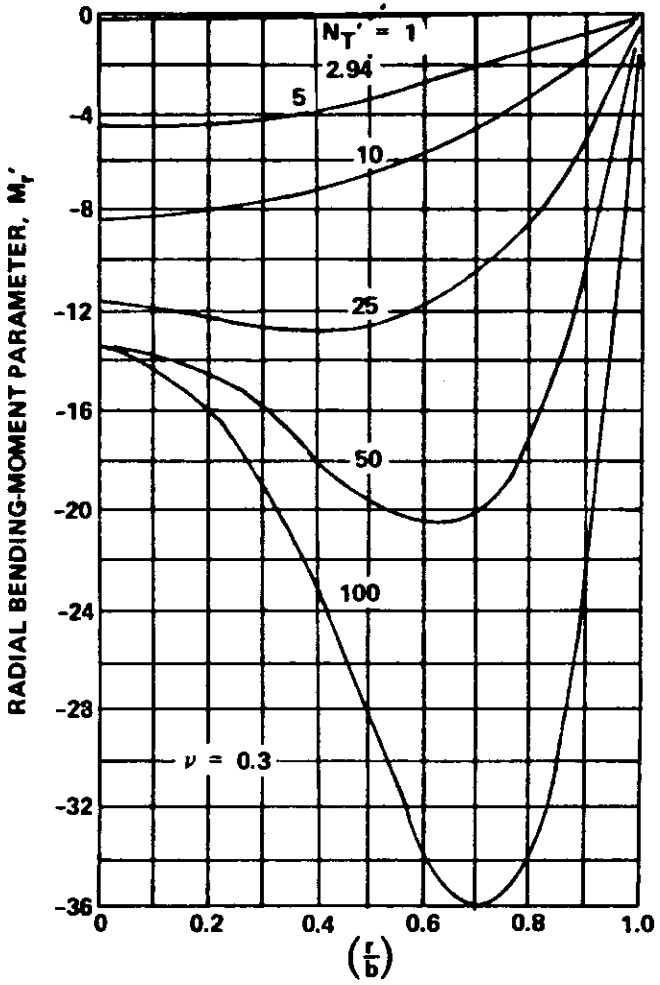

Figure 4.0-4. Nondimensional radial bending-moment parameter.

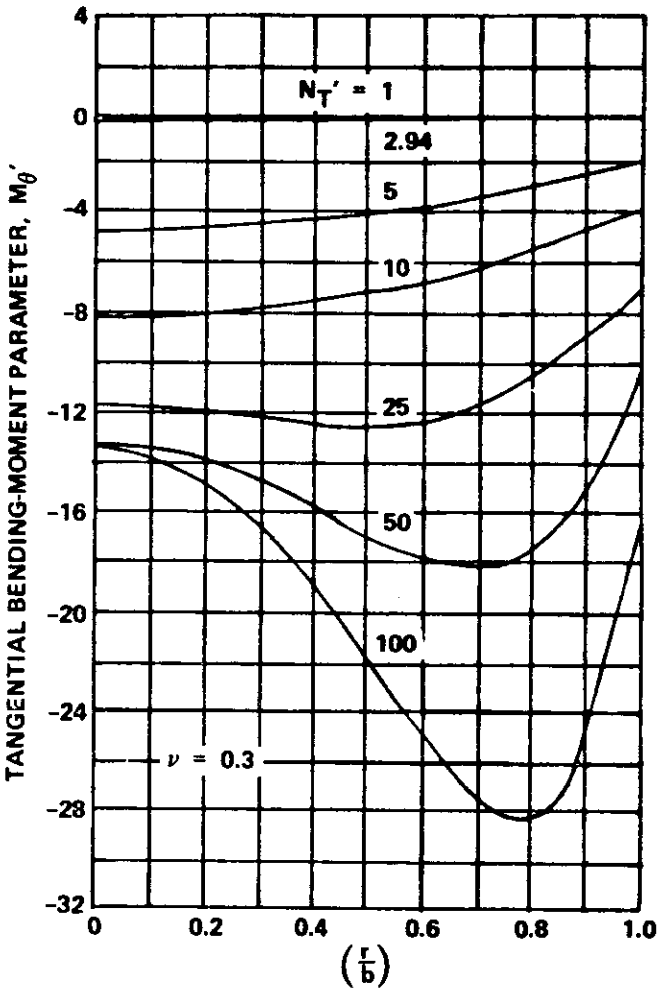

Figure 4.0-5. Nondimensional tangential bending-moment parameter.

$$(\sigma_r)_{cr} = (2.05)^2 \frac{D_b}{b^2 t} \quad . \tag{11}$$

For the thermal problem, the compressive stress just before buckling is given by

$$\sigma_r = \frac{-N_T}{t(1-\nu)} \tag{12}$$

where

$$N_T = E\alpha \int_{-t/2}^{t/2} T \, dz \quad . \tag{13}$$

From equations (11) and (12), the critical nondimensional value for N_T at buckling is given by

$$(N_T')_{cr} = (N_T)_{cr} \frac{b^2}{D_b} = 2.94 \quad . \tag{14}$$

Equation (14) shows that initial buckling of the plate will occur when $N_T' = 2.94$, provided that $\nu = 0.3$. Hence, when $N_T' < 2.94$, the plate will remain flat and the deflection w, as well as the bending moments M_r and M_θ, must equal zero. An inspection of equations (17) and (18) together with Figures 4.0-4 and 4.0-5 reveals that this requirement is essentially satisfied by the given method.

The deflection pattern of the buckled plate will consist of an axisymmetric bulge which can occur in either the upward or downward direction. In actual practice, the direction will be determined by the type of initial

imperfections present in the plate, the nature of external disturbances, etc. The formulas and design curves associated with the deflections and the bending moments are based on the assumption that the plate deflects downward. On the other hand, the sense of the membrane forces (compressive versus tensile) at any point will be independent of the bulge direction. Hence, the expressions for N_r and N_θ, taken in conjunction with Figures 4.0-2 and 4.0-3, are valid for both types of deformation.

It is assumed that Young's modulus and Poisson's ratio are unaffected by temperature variations. On the other hand, the temperature-dependence of the thermal-expansion coefficient can be accounted for by recognizing that it is the product αT which governs; that is, the actual temperature distribution can be suitably modified to compensate for variations in α.

It should be noted that there is a typographical error in equation (5) of Ref. 32 where the quantity $(1 - \nu)^2$ should be changed to $(1 - \nu^2)$. The contents of this section have been corrected accordingly.

Example Problems.

For the first example problem, consider a circular steel plate which is 0.10 in. in thickness and has an outer radius a of 10.0 in. The outer edges are fully restrained against in-plane expansion; however, they are simply supported otherwise. The plate is heated such that the temperature gradient is given by

$$T = 3.0 + 6.0\,(z/t)^2 \quad .$$

Using $\alpha = 6.0 \times 10^{-6}$ in./(in.) (°F), $\nu = 0.30$, and $E = 30.0 \times 10^6$ psi, determine whether buckling has occurred and find the stresses and deflections. From equations (16)

$$N_T' = \frac{12(1-\nu^2)\, b^2}{Et^3} E\alpha \int_{-t/2}^{t/2} [3.0 + 6.0\,(z/t)^2]\, dz \quad ,$$

$$N_T' = \frac{12(1.0-0.09)(10.0)^2}{(30.0 \times 10^6)(0.10^3)} (30.0 \times 10^6)(6.0 \times 10^{-6}) \left[3.0(z) + \frac{6.0(z^3)}{(t^2)3} \right]_{-t/2}^{t/2} \quad ,$$

$$N_T' = 6.55 \left[3.0\left(\frac{t}{2} + \frac{t}{2}\right) + \frac{2.0}{(t^2)} \left(\frac{t^3}{8} + \frac{t^3}{8}\right) \right] = 6.55(3.5)(t) \quad ,$$

and

$$N_T' = 2.29 \quad .$$

Since this is less than the critical buckling value given by equation (14), the plate has not buckled and thus the deflection, as well as the bending moments M_r and M_θ, are equal to zero.

However, from an inspection of equations (17) for the stresses and knowing that, for $N_T' = 2.29$, $M_r' = M_\theta' = 0$ and the values of N_r' and N_θ' can be obtained from Figures 4.0-2 and 4.0-3 as a function of (r/b), the stresses may be easily calculated by inserting the appropriate values in the equations.

For a second example use the same plate as for the first; however, apply a temperature gradient to the plate as follows:

$$T = 33.0 + 66.0(z/t)^2 \quad .$$

For this thermal loading

$$N_T' = 6.55\,[33.0(t) + 5.5(t)] = 6.55(38.5)(0.10) = 25.2 \quad .$$

Since this is greater than the critical buckling value of 2.94, as given in equation (15), the plate has buckled. Then, using Figures 4.0-1 through 4.0-5 the deflections, stress resultants and moments may be obtained for the calculated value of N_T'. These values may then be substituted into equations (17) to obtain the stresses and deflections. For this problem assume that the stresses and deflections are needed for values of (r/b) = 0.3 and = 0.6. Then, on the basis of $N_T' = 25.2$, the following table gives values for the terms needed in the stress and deflection calculations.

r/b	w' (Fig. 4.0-1)	N_r' (Fig. 4.0-2)	N_θ' (Fig. 4.0-3)	M_r' (Fig. 4.0-4)	M_θ' (Fig. 4.0-5)
0.30	1.75	1.40	-1.20	-12.70	-12.30
0.60	1.20	-1.70	-10.00	-12.00	-12.40

Setting up equations (17) for calculation of the stresses and deflections for this problem,

$$w = w'(t) = 0.10(w')$$

and

$$\sigma_r = \left[\frac{-12z\,(M_r')}{t\sqrt{6(1-\nu^2)}} + \frac{(N_T')}{(1-\nu)} - 12(1+\nu)\left(\frac{b^2}{t^2}\right)\alpha T + (N_r') \right] \frac{D_b}{b^2 t} \quad .$$

Letting $z = t/2$; $T = [33.0 + 66.0(0.5)^2] = 49.5$,

$$\frac{D_b}{b^2 t} = \frac{30.0 \times 10^6 \times (0.10)^3}{12(1.0 - 0.09)\ (10.0)^2\ (0.10)} = 2750.0 \quad .$$

Then,

$$\sigma_r = 2750.0 \left[\frac{-12(0.5t)(M_r')}{t\sqrt{6(1.0 - 0.09)}} + \frac{25.2}{(1.0 - 0.3)} \right.$$

$$\left. - 12(1.0 + 0.3) \left(\frac{10.0}{0.10}\right)^2 (6.0 \times 10^{-6}\ (49.5) + (N_r') \right],$$

$$\sigma_r = [-7060\ (M_r') + 99\,000 - 127\,320 + 2750\ (N_r')] \quad ,$$

and

$$\sigma_r = [-7060(M_r') + 2750\ (N_r') - 28\,320] \quad .$$

Also,

$$\sigma_\theta = [-7060\ (M_\theta') + 2750\ (N_\theta') - 28\,320] \quad .$$

Then, for (r/b) = 0.30,

$$w = 0.10\ (w') = 0.10\ (1.75) = 0.175 \text{ in.}$$

and

$$\sigma_r = -7060\ (-12.70) + 2750\ (1.40) - 28\,320$$

$$= +80\,660 + 3850 - 28\,320 = +65\,190 \text{ psi} \quad .$$

Similarly,

$$\sigma_\theta = +55\,220 \text{ psi} \quad \text{(Note that these are tension stresses.)}$$

for (r/b) = 0.60 .

As before,

$$w = 0.120 \text{ in.},$$

$$\sigma_r = + 51\ 720 \text{ psi},$$

and

$$\sigma_\theta = + 31\ 720 \text{ psi} \quad .$$

The previously calculated stresses represent the critical tension values. Critical compression stresses are found by letting $z = - t/2$ in the first stress term. Then

$$\sigma_r = [7060\ (M_r') + 2750\ (N_r') - 28\ 320]$$

and

$$\sigma_\theta = [7060\ (M_\theta') + 2750\ (N_\theta') - 28\ 320] \quad .$$

The following table gives the critical tensile and compressive stresses and deflections at the plate stations.

(r/b)	w (in.)	Tensile Stress (psi)		Compressive Stress (psi)	
		σ_r	σ_θ	σ_r	σ_θ
0.30	0.175	+65 190	+55 220	-114 130	-118 460
0.60	0.125	+51 720	+31 720	-117 720	-143 360

Summary of Equations and Curves.

Critical Condition for Buckling.

$$(N_T')_{cr} = (2.94)_{\nu = 0.3} \qquad (15)$$

where

$$N_T' = \frac{N_T b^2}{D_b} = E\alpha \left(\int_{-t/2}^{t/2} T \, dz \right) \frac{b^2 12(1 - \nu^2)}{Et^3} ,$$

$$D_b = \frac{Et^3}{12(1 - \nu^2)} , \tag{16}$$

and

$$N_T = E\alpha \int_{-t/2}^{t/2} T \, dz.$$

Postbuckling Deflections and Stresses.

$$w = w' t$$

$$\sigma_r = \left[- \frac{12 z M_r'}{t\sqrt{6(1 - \nu^2)}} + \frac{N_T'}{(1 - \nu)} - 12(1 + \nu) \frac{b^2}{t^2} \alpha T + N_r' \right] \frac{D_b}{b^2 t} \tag{17}$$

and

$$\sigma_\theta = \left[- \frac{12 z M_\theta'}{t\sqrt{6(1 - \nu^2)}} + \frac{N_T'}{(1 - \nu)} - 12(1 + \nu) \frac{b_2}{t^2} \alpha T + N_\theta' \right] \frac{D_b}{b^2 t}$$

where

$$M_r' = - \frac{M_r b^2}{D_b t} \sqrt{6(1 - \nu^2)} ,$$

$$M_\theta' = - \frac{M_\theta b^2}{D_b t} \sqrt{6(1 - \nu^2)} , \tag{18}$$

$$N_r' = \frac{N_r b^2}{D_b} ,$$

and

$$N_\theta' = \frac{N_\theta b^2}{D_b} .$$

The values for w', M_r', M_θ', N_r', and N_θ' are obtained from Figures 4.0-1 through 4.0-5 for the case of $\nu = 0.3$.

For values of ν other than 0.3, the values of M_r' and M_θ' may be found by using equations (18) as shown:

$$(M_r')_\nu = \left[(M_r')_{\nu = 0.3}\right] \sqrt{\frac{(1 - \nu^2)}{(1.0 - 0.3^2)}} = 1.049 \sqrt{(1 - \nu^2)}\,(M_r')_{\nu = 0.3} .$$

Similarly,

$$(M_\theta')_\nu = 1.049 \sqrt{(1 - \nu^2)}\,(M_\theta')_{\nu = 0.3} .$$

N_r' and N_θ' are independent of ν.

4.0.2.2 Rectangular Plates

I. Heated Plates Loaded in Plane — Edges Unrestrained in the Plane.

Consider the plate strip, shown on the following page, loaded at the ends by a uniformly distributed stress σ_0, subjected to a uniformly distributed heat input Q, and reinforced along the edges ($y = 0$, $y = b$) by longitudinals. The temperature in the plate will be higher in the center of the panel than near the edges because of the heat sink provided by the longitudinals. For the present purposes the temperature will be taken to be uniform across the thickness and of the form

$$T = T_0 - T_1 \cos\left(\frac{2\pi y}{b}\right) \qquad (19)$$

in the plane of the plate, where T_0 and T_1 are constants to be adjusted to fit the available data.

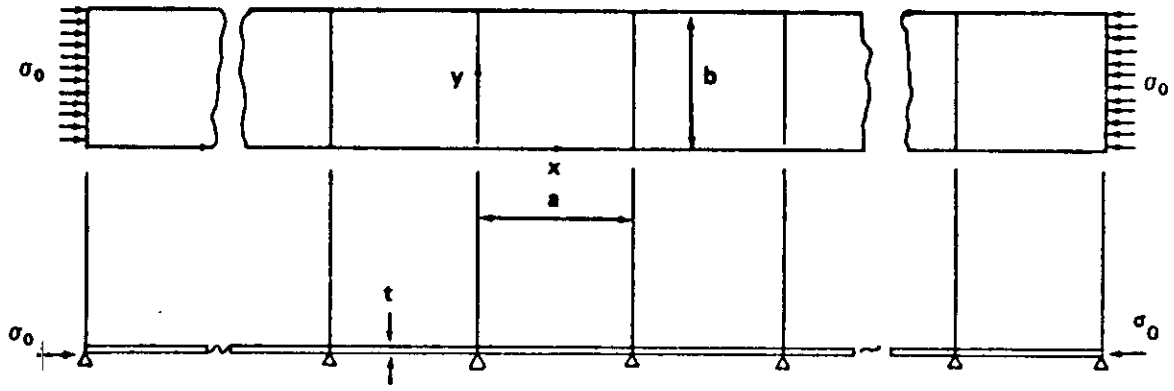

The following solution pertains to a single panel of the strip, extending from x = 0 to x = a. This panel is assumed to be at a sufficient distance from the ends of the strip, so that the stresses may be taken to be independent of x. Transverse displacements are prevented at x = 0, a.

From the solution in Ref. 1 the critical combination of σ_0 and T_1 (note: T_0 has no effect on buckling) is found by obtaining the determinant of simultaneous equations. It was shown that the symmetric case corresponds to the lower buckling load and that the problem can be solved approximately by the interaction of two special cases. These cases are (1) $T_1 = 0$ and σ_0 is acting alone and (2) $\sigma_0 = 0$ and T is acting alone.

The solution to (1) is the standard plate buckling expression found in Ref. 1; that is, when $T_1 = 0$,

$$\sigma_{cr_0} = - \frac{k \pi^2 E}{12(1 - \nu^2)} \left(\frac{t}{b}\right)^2 \qquad (20)$$

where

$$k = 4 \text{ for } \frac{a}{b} \geq 1$$

and

$$k = \left(\frac{b}{a} + \frac{a}{b}\right)^2 \quad \text{for } \frac{a}{b} \leq 1 \quad .$$

The solution to (2) when $\sigma_0 = 0$ is as follows. The critical value of $T_1 (= T_{cr_0})$.

$$\frac{\alpha E T_{cr_0}}{2} = \frac{k_1 \pi^2 E}{12(1 - \nu^2)} \left(\frac{t}{b}\right)^2 \qquad (21)$$

where k_1 is determined from Figure 4.0-6.

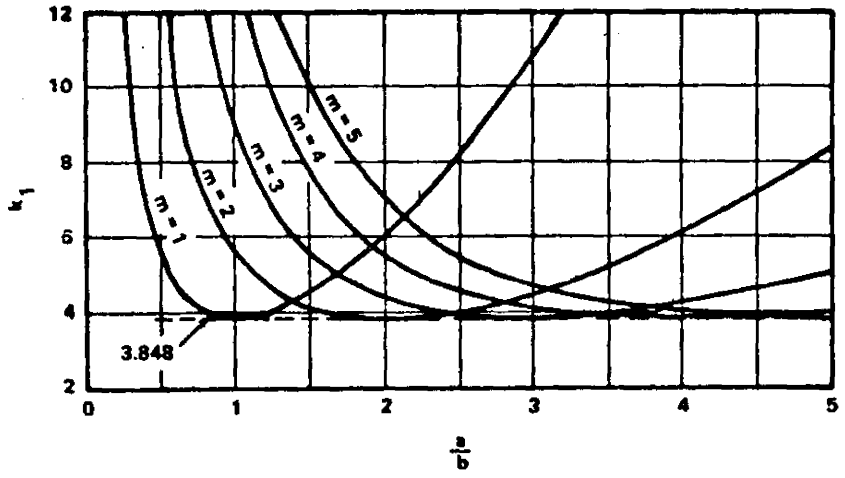

Figure 4.0-6. Values of the coefficient k_1.

Then, for the general case in which both heat and edge stresses are acting, the following interaction curve is used:

$$\frac{T_{cr}}{T_{cr_0}} + \frac{\sigma_{cr}}{\sigma_{cr_0}} = 1 \quad . \qquad (22)$$

II. Heated Plates Loaded in Plane — Edges Restrained in the Plane.

A. Configuration.

The design curves presented here apply only to flat, rectangular plates which are of constant thickness and are made of isotropic material. It is assumed that the plste is free of holes and that no stresses exceed the elastic limit. The edge support members must have the same coefficient of thermal expansion as the plate proper. The design curves cover aspect ratios a/b from 1 through 4. However, since these plots become quite flat at a/b = 4, they must be used to obtain approximate results for aspect ratios greater than 4.

B. Boundary Conditions.

Solutions are given for each of the following two types of boundary conditions:

1. Type I — The boundaries satisfy both the following conditions:

a. All edges of the plate are simply supported.

b. The edge supports fully restrain in-plane plate displacements such that these displacements are equal to the free thermal expansions (or contractions) of the supports.

2. Type II — The boundaries satisfy both of the following conditions:

a. All edges of the plate are clamped.

b. The supports fully restrain in-plane edge displacements of the plate such that these displacements are equal to the free thermal expansions (or contractions) of the supports.

C. Temperature Distribution.

It is assumed that no thermal gradients exist through the plate thickness. The following three types of temperature distributions over the surface are considered and are illustrated in Figure 4.0-7:

1. Sinusoidal distributions which can be expressed mathematically as

$$T = T_o + T_1 \sin\frac{\pi x}{a} \sin\frac{\pi y}{b} \quad . \tag{23}$$

2. Parabolic distributions which can be expressed mathematically as

$$T = T_o + T_1 \left[1 - \left(\frac{2x}{a} - 1\right)^2\right]\left[1 - \left(\frac{2y}{b} - 1\right)^2\right] \quad . \tag{24}$$

3. Tent-like distributions which can be expressed mathematically as

$$T = T_o + T_1 \left[1 - \left(\frac{2x}{a} - 1\right)\right]\left[1 - \left(\frac{2y}{b} - 1\right)\right] \quad . \tag{25}$$

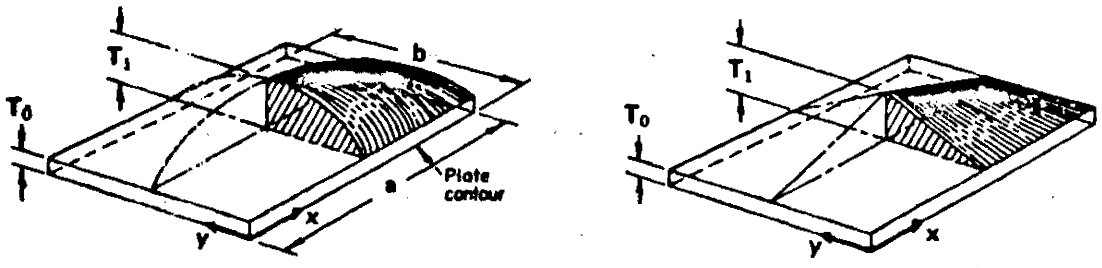

a. Sinusoidal or parabolic distribution.

b. Tent-like distribution.

Figure 4.0-7. Selected temperature distributions over the surface of a rectangular plate.

D. Design Curves.

In Ref. 36 Forray and Newman present the simple means given here to compute the critical temperature values for the initial thermal buckling of flat, rectangular plates. Curves are given for the combinations of boundary conditions and temperature distributions tabulated in Table 4.0-1. The temperature variations were chosen to be representative of what would be expected if the panel were subjected to rapid heating. This condition is conducive to thermal buckling since it will usually cause the plate to be much hotter than the supports. The results of Forray and Newman are plotted in Figure 4.0-8 for plates having $\nu = 0.3$. The curves do not account for nonuniformities in the material properties such as those variations that arise because of temperature-dependence of the material behavior. Hence, the user must select a single effective value for α by employing some type of averaging technique.

TABLE 4.0-1. COMBINATIONS OF BOUNDARY CONDITIONS AND TEMPERATURE DISTRIBUTIONS

Boundary Conditions	Type I	Type II
Temperature Distributions Over the Surface	Sinusoidal	--
	Parabolic	Parabolic
	Tent-Like	--

A nondimensional plot of the deflection at the center of rectangular plates of various aspect ratios against temperature level is presented in Figure 4.0-9 where

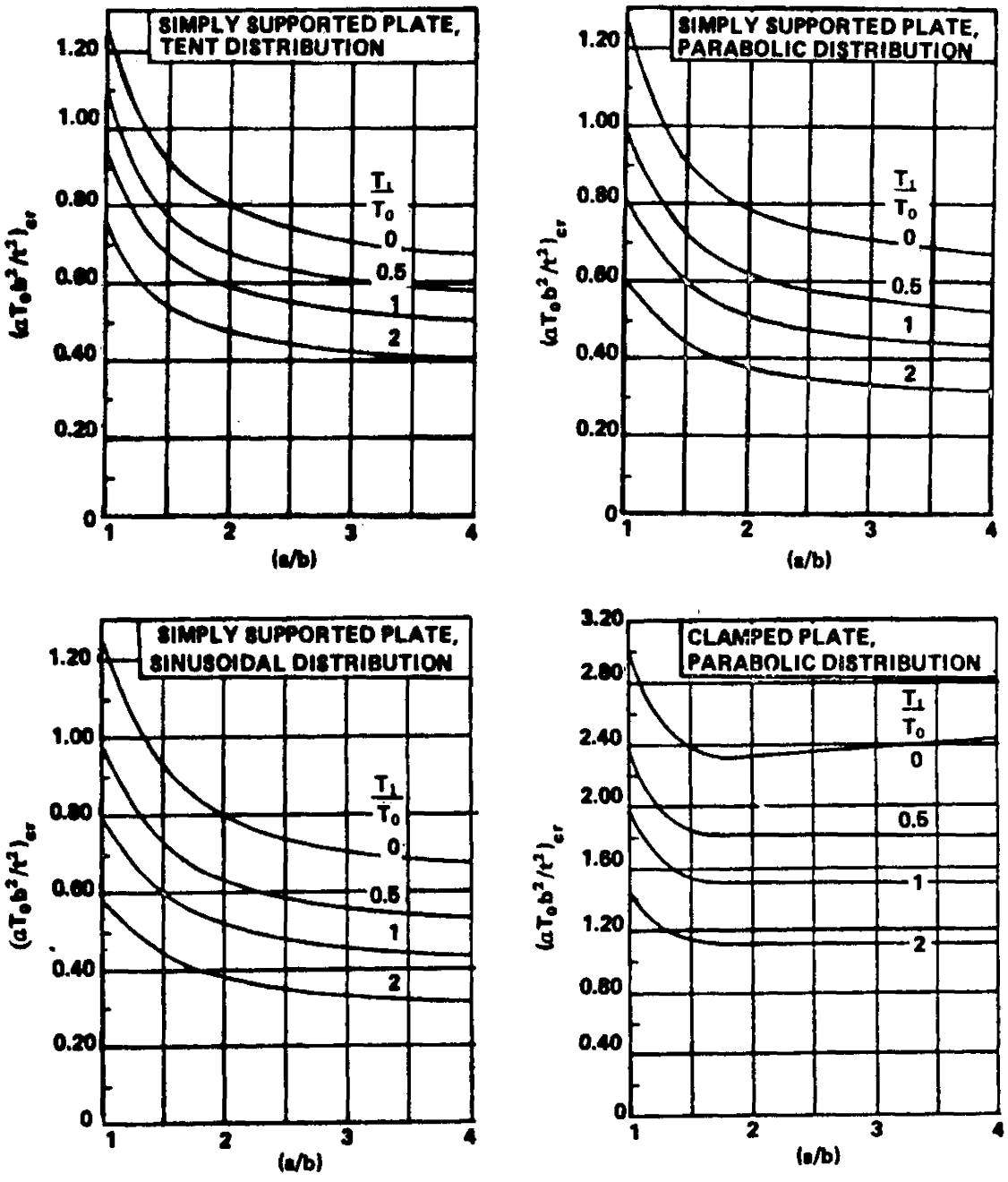

Figure 4.0-8. Critical temperature parameter for rectangular plates.

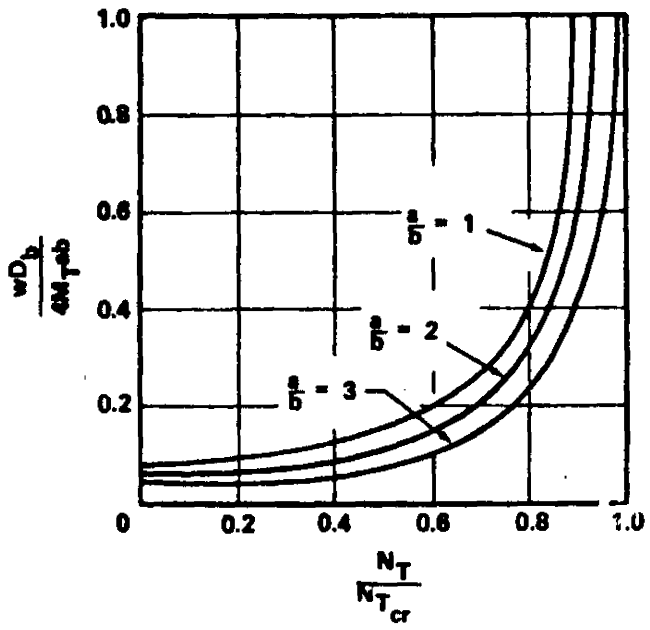

Figure 4.0-9. Deflection w at the center of a rectangular plate for loads in plane of plate $\left(\text{Poisson's ratio } \nu = \frac{1}{4}\right)$.

$$N_T = \alpha E \int_{-t/2}^{t/2} T \, dz, \tag{26}$$

$$M_T = \alpha E \int_{-t/2}^{t/2} Tz \, dz, \tag{27}$$

and

$$D_b = \frac{Et^3}{12(1 - \nu^2)} .$$

In this figure, the nondimensional parametric indicating the temperature level is $\left(N_T/N_{T_{cr}}\right)$, where $N_{T_{cr}}$, the value of N_T at which buckling occurs, is

$$N_{T_{cr}} = (1 - \nu)\left(1 + \frac{a^2}{b^2}\right)\frac{\pi^2 D_b}{a^2} \quad . \tag{28}$$

Plots showing in nondimensional form the variation of M_x in one quadrant of a square plate and presented in Figures 4.0-10 and 4.0-11 for two different temperature levels. Because of the double symmetry of the plate, such a plot is sufficient to determine the distribution of both M_x and M_y throughout the entire plate. These plots indicate that the maximum bending moment occurs, for the cases considered, in the center of the plate. Curves showing the variation of center moment with temperature level for various aspect ratios are shown in Figure 4.0-12.

It should be noted that the preceding results were obtained on the assumption that nonlinear terms in the strain-displacement relations could be neglected. Therefore, as is usual in problems of this type, the results are valid only for values of N_T sufficiently small relative to $N_{T_{cr}}$.

III. Post-Buckling Deflections With All Edges Simply Supported.

A. Configuration.

The design curves presented here apply only to flat, rectangular plates which are of constant thickness and are made of isotropic material. It is assumed that the plate is free of holes and that no stresses exceed the elastic limit. The edge support members must have the same coefficient of thermal expansion as the plate proper. The design curves cover aspect ratios a/b of 1, 2, 3, and $a/b \geq 5$.

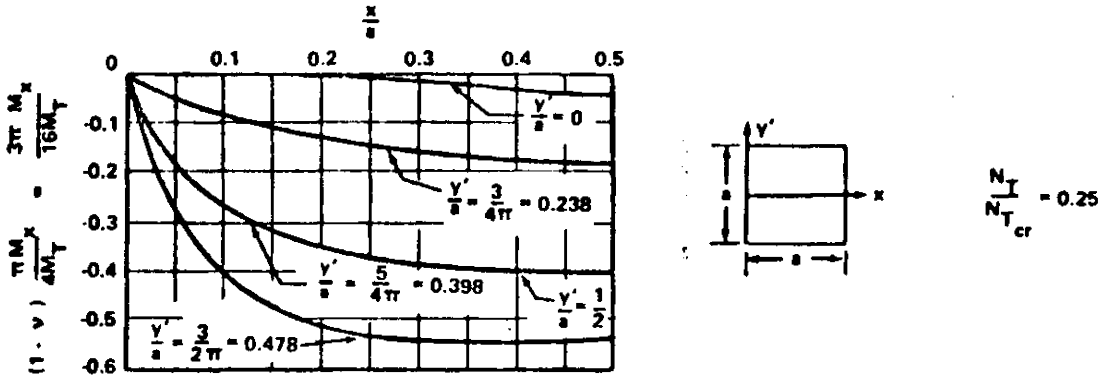

Figure 4.0-10. Distribution of the bending moment M_x in a square plate for

$$\frac{N_T}{N_{T_{cr}}} = 0.25 \quad \left(\text{Poisson's ratio } \nu = \frac{1}{4}\right) .$$

B. Boundary Conditions.

The solution applies only to cases where both the following boundary conditions are satisfied:

1. All edges are simply supported.

2. Supports fully restrain in-plane edge displacement of the plate such that these displacements are equal to the free thermal expansions (or contractions) of the supports.

C. Temperature Distribution.

It is assumed that no thermal gradients exist through the plate thickness. Temperature distribution over the surface is taken to be parabolic (Fig. 4.0-13) and can be expressed mathematically as

$$T = T_o + T_1\left[1 - \left(\frac{2x}{a} - 1\right)^2\right]\left[1 - \left(\frac{2y}{b} - 1\right)^2\right] . \qquad (29)$$

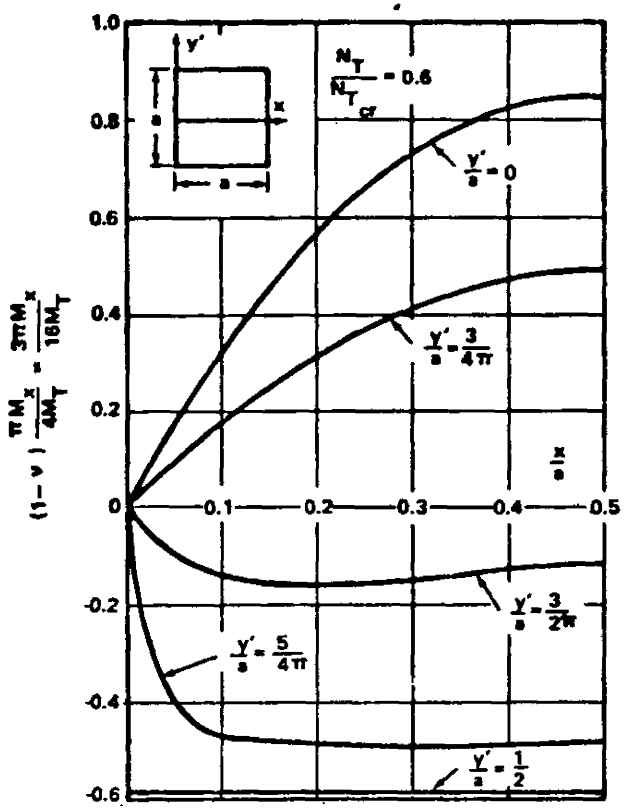

Figure 4.0-11. Distribution of the bending moment M_x in a square plate for $\frac{N_T}{N_{T_{cr}}} = 0.6$ $\left(\text{Poisson's ratio } \nu = \frac{1}{4}\right)$.

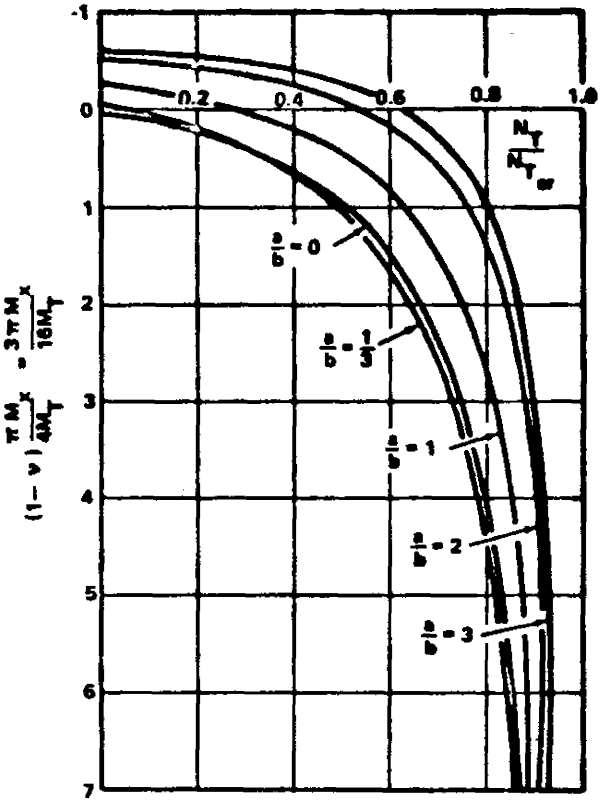

Figure 4.0-12. Bending moment M_x at the center of a rectangular plate.

D. Design Curves.

In many aerospace applications, thermal buckling of flat, rectangular plates can be tolerated if the post-buckling deflections do not cause excessive losses of aerodynamic efficiency, do not produce destructive aerodynamic disturbances, etc. In Ref. 37, Newman and Forray present the simple means given as follows to compute absolute values of the maximum post-buckling deflections for such plates. The temperature variation was chosen to be representative of what would be expected when the panel is subjected to rapid heating. This condition is conducive to thermal buckling since it will usually cause the plate to be much hotter than the supports.

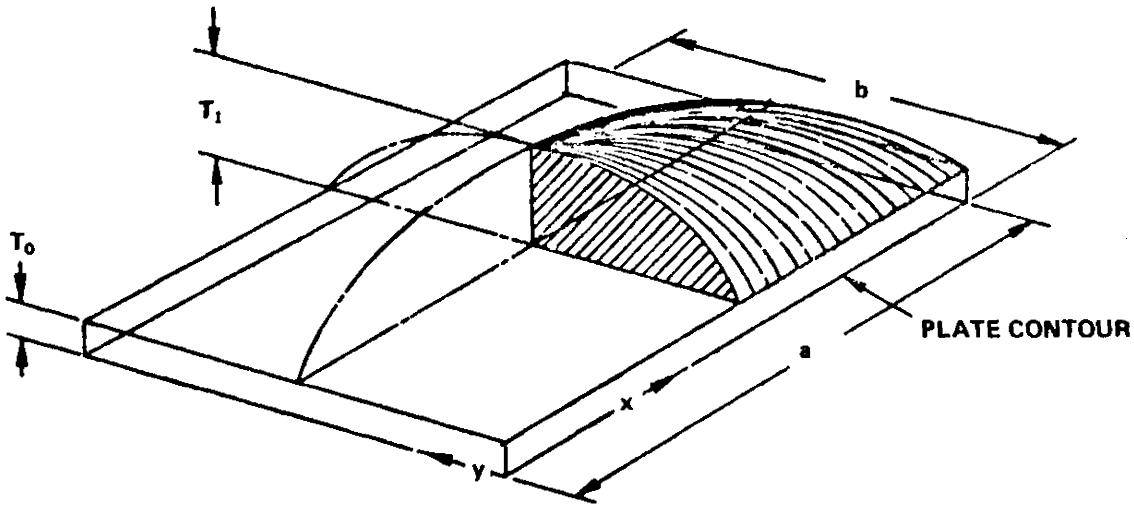

Figure 4.0-13. Parabolic temperature distribution over the surface of a rectangular plate.

The maximum post-buckling deflection occurs at the center of the plate and can be calculated from the relationship

$$\frac{T_1}{\beta} = \frac{\pi^2}{24}\left[\frac{K^2 + \frac{3}{4}\left[(3-\nu^2)\left(1+\frac{b^4}{a^4}\right) + 4\nu\left(\frac{b^2}{a^2}\right)\right]\frac{\delta^2}{t^2}}{\left(\frac{2}{1-\nu}\right)(K)\left(\frac{T_o}{T_1}+\frac{4}{9}\right) + \left(\frac{8}{3\pi^2}\right)(K)}\right] \qquad (30)$$

where

$$K = 1 + \frac{b^2}{a^2} \qquad (31)$$

and

$$\beta = \frac{1}{\alpha\,(1-\nu^2)}\left(\frac{t}{b}\right)^2 . \qquad (32)$$

Solutions to equation (30) are plotted in Figures 4.0-14 and 4.0-15 for plates having $\nu = 0.30$. It is useful to note that, for given values of T_0/T_1, initial thermal buckling occurs at T_1/β values corresponding to $\delta/t = 0$. The curves do not account for nonuniformities in the material properties such as those variations that arise because of temperature-dependence of the material behavior. Hence, the user must select a single effective value for α by employing some type of averaging technique.

4.0.3 Thermal Buckling of Cylinders.

Configuration.

The design curves and equations provided here apply only to thin-walled, right circular cylinders which satisfy the relationship

$$L/R \geq \frac{3.2}{\left(\frac{R}{t}\right)^{1/2}} \qquad (33)$$

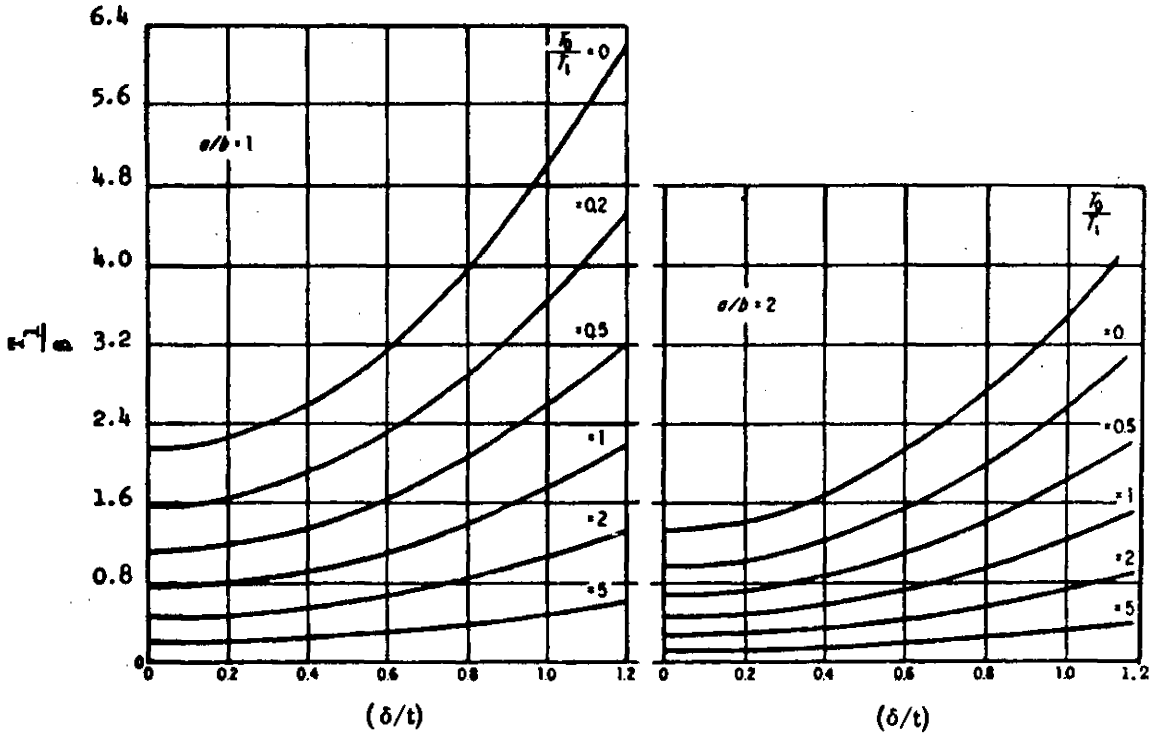

Figure 4.0-14. Post-buckling parameters for heated rectangular plates.

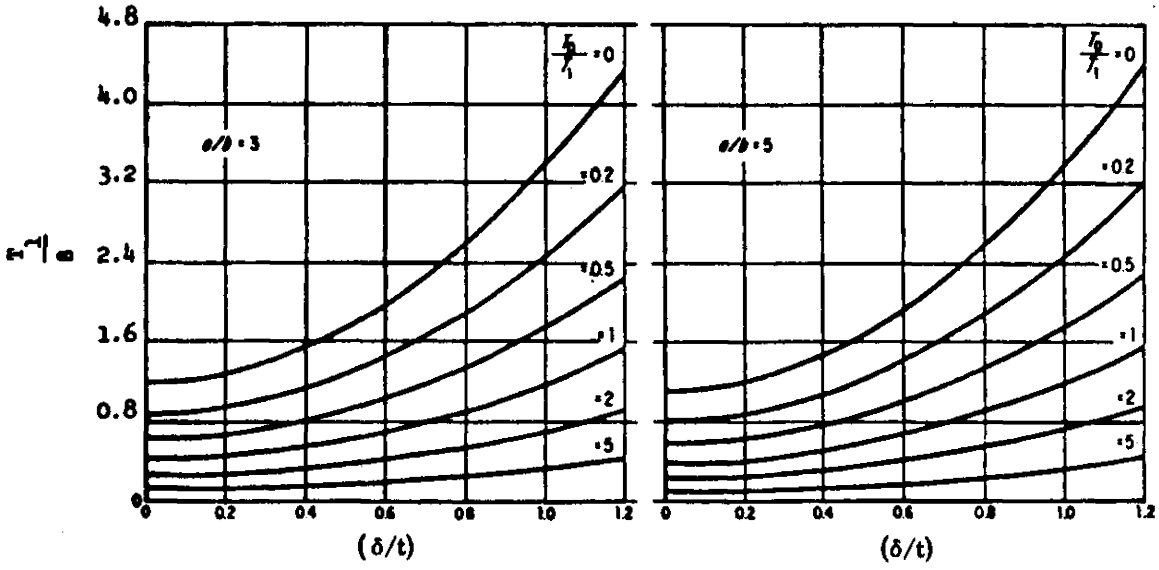

Figure 4.0-15. Post-buckling parameters for heated rectangular plates.

and are made of isotropic material. It is assumed that the shell wall is free of holes, obeys Hooke's law, and is of constant thickness. Figure 4.0-16 depicts the isotropic cylindrical shell configuration. Figure 4.0-17 shows the sign convention for forces, moments, and pressures.

Boundary Conditions.

The following types of boundary conditions are covered:

1. Simply supported edge; that is,

$$w = M_x = 0 \quad \text{at } x = 0 \text{ and/or } x = L. \tag{34}$$

2. Clamped edge; that is,

$$w = \frac{\partial w}{\partial x} = 0 \quad \text{at } x = 0 \text{ and/or } x = L \quad . \tag{35}$$

It is not required that the conditions at the two ends be the same. In every case, it is assumed that the cylinder (including any end rings) is not subjected to external axial constraints at any location around the boundaries at $x = 0$ and $x = L$.

Temperature Distribution.

The supposition is made that no thermal gradients exist through the wall thickness and in the axial direction. However, arbitrary circumferential variations may be present. The permissible distributions can therefore be expressed in the form

$$T = T(\phi) \quad . \tag{36}$$

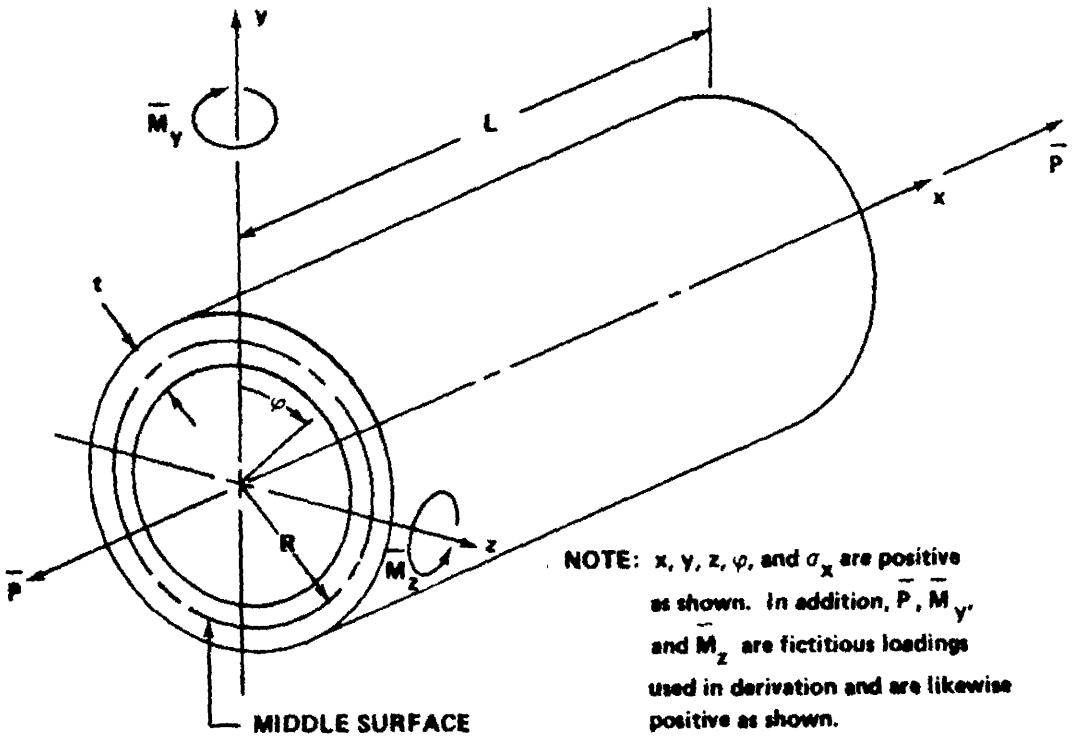

Figure 4.0-16. Isotropic cylindrical shell configuration for thermal buckling.

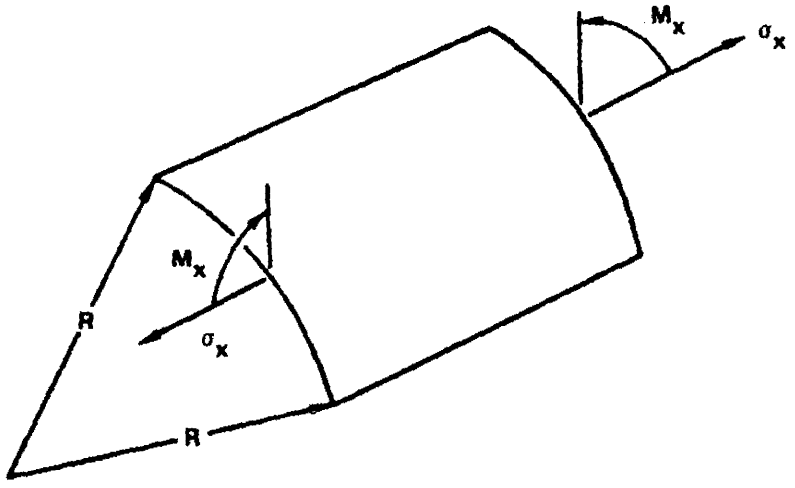

Figure 4.0-17. Sign convention for forces, moments, and pressure for thermal buckling.

Hoop membrane compression may develop in regions adjacent to the two ends because of external radial constraint. However, the buckling mode associated with this condition is not considered. Because of this and the lack of external axial constraints, the special case of a uniform temperature is of no interest here.

Design Curves and Equations.

It is assumed that Young's modulus and Poisson's ratio are unaffected by temperature changes. Hence, in using the contents of this manual, the user must select effective values for each of these properties by applying engineering judgement. It will sometimes be desirable to employ different effective moduli in each of the following operations:

1. Computation of the stresses σ_x present in the cylinder
2. Computation of the critical buckling stress $(\sigma_x)_{cr}$.

On the other hand, the results are presented in a form which enables the user to fully account for temperature-dependence of the thermal-expansion coefficient α .

The appropriate formulation for σ_x can be obtained by first imposing a fictitious stress distribution σ_A around the boundaries at $x = 0$ and $x = L$ such that all axial thermal deformations are entirely suppressed. It follows that

$$\sigma_A = - \alpha \, E T \, (\phi) \quad . \tag{37}$$

These stresses may be integrated around the circumference and through the wall thickness to arrive at the force

$$\overline{P}_A = - EtR \int_0^{2\pi} \alpha T(\phi) \, d\phi \tag{38}$$

and the moments

$$(\overline{M}_y)_A = - ER^2t \int_0^{2\pi} \alpha T(\phi) \sin \phi \, d\phi$$

and (39)

$$(\overline{M}_z)_A = - ER^2t \int_0^{2\pi} \alpha T(\phi) \cos \phi \, d\phi \quad .$$

Since it is assumed that the shell is free of external axial constraints, the conditions

$$\overline{P} = \overline{M}_y = \overline{M}_z = 0 \tag{40}$$

must be satisfied at x = 0 and x = L. To restore the shell to such a state, it is necessary to superimpose a force $\overline{P}_B$ equal and opposite to $\overline{P}_A$ as well as moments $(\overline{M}_y)_B$ and $(\overline{M}_z)_B$, which are equal and opposite to $(\overline{M}_y)_A$ and $(\overline{M}_z)_A$, respectively. Hence,

$$\overline{P}_B = - \overline{P}_A ,$$

$$(\overline{M}_y)_B = - (\overline{M}_y)_A , \tag{41}$$

and

$$(\overline{M}_z)_B = -(\overline{M}_z)_A \quad .$$

The stress corresponding to $\overline{P}_B$ is easily found to be

$$\left(\sigma_{\overline{P}}\right)_B = \frac{\overline{P}_B}{A} = \frac{\overline{P}_B}{2\pi Rt} = \frac{E}{2\pi}\int_0^{2\pi} \alpha T(\phi)\, d\phi \quad . \tag{42}$$

The stresses due to $(\overline{M}_y)_B$ are

$$\left(\sigma_{\overline{M}_y}\right)_B = \frac{(\overline{M}_y)_B z}{I_y} = \frac{(\overline{M}_y)_B z}{\pi R^3 t} = \frac{E \sin\phi}{\pi}\int_0^{2\pi} \alpha T(\phi) \sin\phi\, d\phi \tag{43}$$

and those due to $(\overline{M}_z)_B$ are

$$\left(\sigma_{\overline{M}_z}\right)_B = \frac{(\overline{M}_z)_B y}{I_z} = \frac{(\overline{M}_z)_B y}{\pi R^3 t} = \frac{E \cos\phi}{\pi}\int_0^{2\pi} \alpha T(\phi) \cos\phi\, d\phi \quad . \tag{44}$$

The procedure being used constitutes an application of Saint-Venant's principle. Hence, the stresses from equations (42) through (44) will be accurate representations only at sufficient distances from the ends x = 0 and x = L. If end rings are present, the greater their resistance to out-of-plane bending, the shorter will be this distance. Subject to these conditions, the actual longitudinal thermal stresses at various points in the shell may be computed from the relationship

$$\sigma_x = \sigma_A + \left(\sigma_{\overline{P}}\right)_B + \left(\sigma_{\overline{M}_y}\right)_B + \left(\sigma_{\overline{M}_z}\right)_B \tag{45}$$

or

$$\sigma_x = -\alpha E T(\phi) + \frac{E}{2\pi}\int_0^{2\pi} \alpha T(\phi)\, d\phi$$

$$+ \frac{E \sin\phi}{\pi}\int_0^{2\pi} \alpha T(\phi) \sin\phi\, d\phi$$

$$+ \frac{E \cos\phi}{\pi}\int_0^{2\pi} \alpha T(\phi) \cos\phi\, d\phi \quad . \tag{46}$$

Complex distributions may be encountered which make it difficult to perform the required integrations. In such instances, use can be made of numerical techniques whereby the integral signs are replaced by summation symbols.

To investigate the stability of a particular shell, the maximum longitudinal stress $(\sigma_x)_{max}$ must be compared against the critical value which can be obtained from the formula

$$(\sigma_x)_{cr} = \gamma \frac{Et}{R\sqrt{3(1-\nu^2)}} \quad . \tag{47}$$

For the design to be satisfactory, it is required that

$$(\sigma_x)_{max} < (\sigma_x)_{cr} \quad . \tag{48}$$

The quantity γ appearing in equation (47) is a so-called knockdown factor, which mainly accounts for the detrimental effects from initial imperfections. Note that equation (47) is identical to that used for uniformly compressed circular, cylindrical shells. Its application to the present problem is justified on the basis of small-deflection studies reported in Refs. 38 and 39. From the results given in these references, it can be concluded that, regardless of the nature of the circumferential stress distribution, classical theoretical instability is reached when the peak axial compressive stress satisfies the expression

$$(\sigma_x)_{max} \approx \frac{Et}{R\sqrt{3(1-\nu^2)}} \quad . \tag{49}$$

In view of this, the values used here for γ were determined from the 99 percent probability (confidence = 0.95) data for uniformly compressed cylinders, as reported in Ref. 40. The resulting γ values are plotted in Figure 4.0-18 for L/R ratios of 0.25, 1.0, and 4.0.

Summary of Equations and Curves.

$$\sigma_x = -\alpha E T(\phi) + \frac{E}{2\pi}\int_0^{2\pi} \alpha T(\phi)\, d\phi$$

$$+ \frac{E \sin\phi}{\pi}\int_0^{2\pi} \alpha T(\phi) \sin\phi\, d\phi$$

$$+ \frac{E \cos\phi}{\pi}\int_0^{2\pi} \alpha T(\phi) \cos\phi\, d\phi \tag{50}$$

and

$$(\sigma_x)_{cr} = \gamma \frac{Et}{R\sqrt{3(1-\nu^2)}} \quad . \tag{51}$$

When $\nu = 0.3$ this gives

$$(\sigma_x)_{cr} = -0.606\,\gamma \frac{Et}{R} \quad . \tag{52}$$

The knockdown factor γ is obtained from Figure 4.0-18.

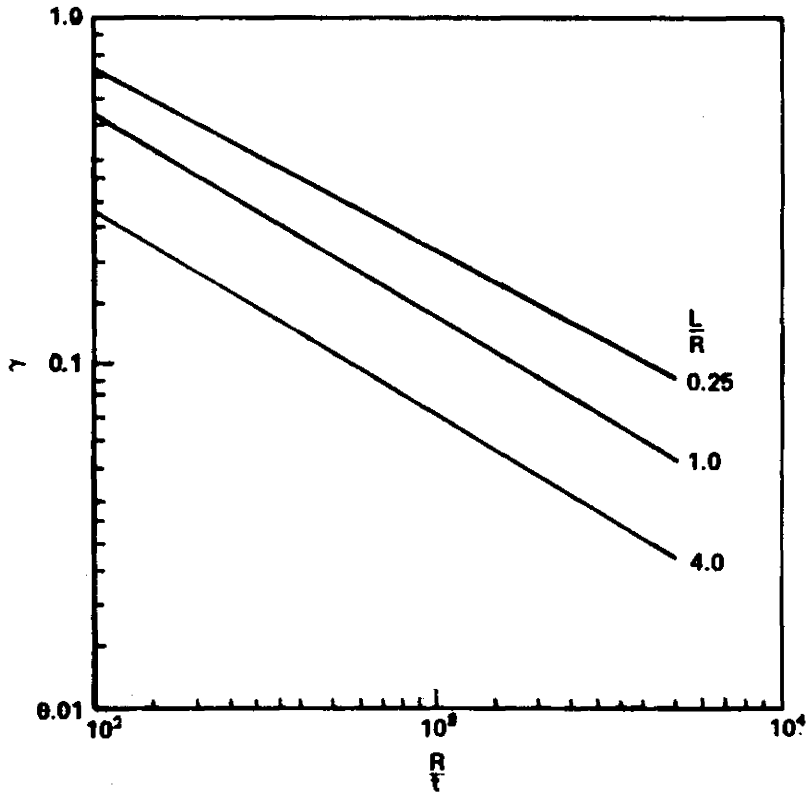

Figure 4.0-18. Knockdown factor.